Inorganic Chemistry
Article

Inorg. Chem. **2010**, *49*, 11297–11308 **11297**
DOI: 10.1021/ic100761f

Synthesis and Characterization of Luminescent Bis-Cyclometalated Platinum^{IV} Complexes

Dustin M. Jenkins[†] and Stefan Bernhard*[,‡]

[†]*Department of Chemistry, Princeton University, Princeton, New Jersey 08540, United States, and*
[‡]*Department of Chemistry, Carnegie Mellon University, Pittsburgh, Pennsylvania 15213, United States*

Received April 20, 2010

Presented is the synthesis and characterization of a series of luminescent heteroleptic bis-cyclometalated platinum^{IV} complexes. An oxidation-facilitated cyclometalation is employed to convert platinum^{II} pendant species into bis-cyclometalated platinum^{IV} dichlorides, which are transformed into the tris-chelated diimine complexes through ligand substitution. The structure−property relationship is probed by judiciously varying substituents on both the C^N and the N^N ligands resulting in a family of complexes exhibiting blue emission, long excited-state lifetimes, and highly efficient oxygen quenching. Excited-state properties are corroborated by static and time-dependent density-functional theory calculations of both the singlet and the triplet state.

Introduction

Ionic transition metal complexes have gained much recognition because of their unique photophysical properties and reversible electrochemical characteristics.[1−5] Square planar and octahedral architectures utilizing second or third row metals and polypyridyl chelates have by far received the most attention and remain at the forefront of current research. The hallmarks of these complexes are long-lived triplet excited states, redox stability, and broad control of emissive and electrochemical attributes through judicious structural modification.[6−10] Such qualities lend them to a wide variety of applications such as optoelectronics,[11−17] sensor technology,[18−23] and photocatalysis.[11,12,24−30]

Since early investigations of exclusively orange-emitting $[Ru(bpy)_3]^{2+}$ complexes, synthetic control over the excited state, and thus the luminescent and electrochemical properties, has been attained. Third row metals such as Os^{II}, Ir^{III}, and Pt^{II}, and stronger field ligands, like the cyclometalating

*To whom correspondence should be addressed. E-mail: bern@cmu.edu.

(1) Juris, A.; Balzani, V.; Barigelletti, F.; Campagna, S.; Belser, P.; Von Zelewsky, A. *Coord. Chem. Rev.* **1988**, *84*, 85.
(2) Baranoff, E.; Yum, J.-H.; Graetzel, M.; Nazeeruddin, Md.K. *J. Organomet. Chem.* **2009**, *694*, 2661.
(3) Slinker, J.; Bernards, D.; Houston, P. L.; Abruña, H. D.; Bernhard, S.; Malliaras, G. G. *Chem. Commun.* **2003**, 2392–2399.
(4) Kvam, P.-I.; Puzyk, M. V.; Balashev, K. P.; Songstad, J. *Acta Chem. Scand.* **1995**, *49*, 335.
(5) Lowry, M. S.; Bernhard, S. *Chem.—Eur. J.* **2006**, *12*(31), 7970.
(6) Son, S. U.; Park, K. H.; Lee, Y.-S.; Kim, B. Y.; Choi, C. H.; Lah, M. S.; Jang, Y. H.; Jang, D.-J.; Chung, Y. K. *Inorg. Chem.* **2004**, *43*, 6896.
(7) Lowry, M. S.; Hudson, W. R.; Pascal, R. A., Jr.; Bernhard, S. *J. Am. Chem. Soc.* **2004**, *126*(43), 14129.
(8) Zhao, Q.; Liu, S.; Shi, M.; Wang, C.; Yu, M.; Li, L.; Li, F.; Yi, T.; Huang, C. *Inorg. Chem.* **2006**, *45*, 6152.
(9) De Angelis, F.; Fantacci, S.; Evans, N.; Klein, C.; Zakeeruddin, S. M.; Moser, J.-E.; Kalyanasundaram, K.; Bolink, H. J.; Graetzel, M.; Nazeeruddin, M. K. *Inorg. Chem.* **2007**, *46*, 5989.
(10) Dragonetti, C.; Falciola, L.; Mussini, P.; Righetto, S.; Roberto, D.; Ugo, R.; Valore, A. *Inorg. Chem.* **2007**, *46*, 8533.
(11) Goldsmith, J. I.; Hudson, W. R.; Lowry, M. S.; Anderson, T. H.; Bernhard, S. *J. Am. Chem. Soc.* **2005**, *127*, 7502.
(12) Lowry, M. S.; Goldsmith, J. I.; Slinker, J. D.; Rohl, R.; Pascal, R. A.; Malliaras, G. G.; Bernhard, S. *Chem. Mater.* **2005**, *17*, 5712.
(13) Gratzel, M. *Inorg. Chem.* **2005**, *44*, 6841.
(14) Moser, J. E.; Bonnote, P.; Gratzel, M. *Coord. Chem. Rev.* **1998**, *171*, 245.
(15) Gratzel, M. *Phil. Trans. R. Soc. A* **2007**, *365*, 993.
(16) He, L.; Duan, L.; Qiao, J.; Wang, R.; Wei, P.; Wang, L.; Qiu, Y. *Adv. Funct. Mater.* **2008**, *18*, 2123.
(17) Costa, R. D.; Orti, E.; Bolink, H. J.; Graber, S.; Schaffner, S.; Neuburger, M.; Housecroft, C. E.; Constable, E. C. *Adv. Funct. Mater.* **2009**, *19*, 3456.
(18) Carraway, E. R.; Demas, J. N.; DeGraff, B. A.; Bacon, J. R. *Anal. Chem.* **1991**, *63*, 337.
(19) Demas, J. N.; DeGraff, B. A.; Coleman, P. B. *Anal. Chem. News & Features* **1999**, 793A.
(20) Kose, M. E.; Carroll, B. F.; Schanze, K. S. *Langmuir* **2005**, *21*, 9121.
(21) Demas, J. N.; DeGraff, B. A. *J. Chem. Educ.* **1997**, *74*(6), 690.
(22) Colvin, A. E.; Phillips, T. E.; Miragliotta, J. A.; Givens, R. B.; Bargeron, C. B. *Johns Hopkins APL Tech. Dig.* **1996**, *17*(4), 377.
(23) Payne, S. J.; Fiore, G. L.; Fraser, C. L.; Demas, J. N. *Anal. Chem.* **2010**, *82*, 917.
(24) Tinker, L. L.; McDaniel, N. D.; Curtin, P. N.; Smith, C. K.; Ireland, M. J.; Bernhard, S. *Chem.—Eur. J.* **2007**, *13*, 8726–8732.
(25) Kalyanasundaram, K.; Kiwi, J.; Grätzel, M. *Helv. Chim. Acta.* **1978**, *61*(7), 2720.
(26) Borgarello, E.; Kiwi, J.; Pelizzetti, E.; Visca, M.; Gratzel, M. *J. Am. Chem. Soc.* **1981**, *103*, 6324.
(27) Cline, E. D.; Adamson, S. E.; Bernhard, S. *Inorg. Chem.* **2008**, *47*(22), 10378.
(28) Krishnan, C. V.; Brunschwig, B. S.; Creutz, C.; Sutin, N. *J. Am. Chem. Soc.* **1985**, *107*, 2005.
(29) (a) Du, P.; Schneider, J.; Fan, L.; Zhao, W.; Patel, U.; Castellano, F. N.; Eisenberg, R. *J. Am. Chem. Soc.* **2008**, *130*, 5056. (b) Brewer, K. J.; Murphy, W. R., Jr.; Moore, K. J.; Eberle, E. C.; Petersen, J. D. *Inorg. Chem.* **1986**, *25*, 2410.
(30) Rau, S.; Schafer, B.; Gleich, D.; Anders, E.; Rudolph, M.; Friedrich, M.; Gorls, H.; Henry, W.; Vos, J. G. *Angew. Chem., Int. Ed.* **2006**, *45*, 6215.

Published on Web 11/24/2010

2-phenylpyridine, have been incorporated to increase ligand field splitting and eliminate thermal population of the nonemissive ^{3}MC state which precludes color tunability in $[Ru(bpy)_3]^{2+}$ and its derivatives.[1,6,8] For instance, cationic bis-cyclometalated Ir^{III} complexes, such as $[Ir(ppy)_2(bpy)]^+$, demonstrate tunability across the visible spectrum and through a wide range of electrochemical potentials,[2,3,5,8,9] and have become key materials in a variety of fields.[8,9,17] The advantages of these complexes in technological applications are numerous. Single-layer OLEDs incorporating ionic transition metal complexes[31,32] demonstrate superior exciton harvesting and, as a result, up to 100% theoretical efficiency,[33−35] turn-on voltages as low as 2.0 V, and can be driven by an alternating current (AC) power supply.[3] Device architectures can be as simple as a luminophore sandwiched between two metal electrodes, fabricated by spin-casting and evaporation onto a glass substrate. Devices exhibiting external quantum efficiencies (EQEs) of up to 16% and power efficiencies of nearly 37 lm/W have already been realized.[36]

Luminescence-based oxygen sensors utilizing ionic transition metal complexes demonstrate high accuracy owing to the long triplet lifetimes and significant oxygen sensitivity of such complexes. Simple devices consisting of an excitation light source, photocell detector, and sensor have been shown to be a promising replacement for the Clark cell since they do not destroy the analyte being measured. The sensor itself usually consists of the luminophore dispersed in an oxygen-permeable polymer or self-assembled monolayer (SAM) membrane and cast onto a surface.[22,37−39]

Moreover, water-reduction systems exploiting ionic transition metal complexes as photosensitizers have received much attention in the past decade as concern grows regarding energy security and the need to utilize alternative fuels such as hydrogen. Most of these systems make use of a noble metal catalyst (such as colloidal platinum) and an amine-based sacrificial reductant in a mixed aqueous/organic solution, illuminated at an appropriate wavelength. Systems exhibiting turnover numbers as high as 5,000 have been reported.[27]

The use of such luminescent metal complexes in the aforementioned applications staunchly supports the continuing interest in these materials. Specifically, the search for blue emitters amenable to application in single-layer OLEDs is ongoing,[3,16,35,39] and the need for highly sensitive oxygen sensors with faster response/recovery times persists. To address some of these issues we have synthesized the first heteroleptic bis-cyclometalated Pt^{IV} complexes of the architecture $[Pt(ppy)_2(bpy)]^{2+}$. Numerous complexes of Pt^{IV} have been explored as anticancer agents[40−43] and in various catalytic reactions,[44,45] but compounds with an octahedral, triply chelated structure have, until now, been unknown. In this work, green and blue emission is readily demonstrated in such complexes through ligand modification, and full spectroscopic, photophysical, and electrochemical characterization is provided alongside a computational treatment of both ground- and excited-states using static and time-dependent density-functional methods. Additionally, particular complexes are shown to exhibit very long lifetimes and high sensitivity to oxygen quenching.

Experimental Section

Materials. Potassium tetrachloroplatinate^{II} and 4,4′-dimethoxy-2,2′-bipyridine were purchased from Aldrich and used as received. 2-Phenylpyridine, ammonium hexafluorophosphate, thallium^{I} nitrate, and silver^{I} trifluoromethanesulfonate were purchased from Alfa Aesar and used as received. 2,2′-Bipyridine was purchased from Acros and used as received.

General Methods. Syntheses of the ligands 5-methyl-2-(4-fluorophenyl)pyridine, 5-methyl-2-(4-methoxyphenyl)pyridine, 5-methyl-2-(biphen-4-yl)pyridine, and 5,5′-difluoro-2,2′-bipyridine, and iodobenzene dichloride are described in the Supporting Information.

Synthesis of Pt^{II} Pendant Complexes. The parent Pt^{II} pendant complexes were synthesized using a procedure similar to that employed by Niedermair et al.[46] The 2-phenylpyridine was combined with potassium tetrachloroplatinate in a mixture of 1:1 *tert*-butanol and water at 80 °C. The precipitate was filtered and washed in methanol for good yields (60−89%). For spectroscopic analyses, fine crystals were obtained using the vapor diffusion of diethyl ether into a solution of the complex in dichloromethane.

Pt(ppy)(ppyH)Cl (1a). 2-Phenylpyridine (0.157 g, 1.011 mmol) was combined with potassium tetrachloroplatinate (0.200 g, 0.482 mmol) in a 1:1 mixture of *tert*-butanol and water (10 mL) at 80 °C for 12 h. The reaction was cooled and the yellow precipitate was filtered and washed in methanol (30 mL) to obtain the pure product (**1a**). Yield: 0.155 g (59.5%). Product confirmed by ^{1}H NMR as previously reported.[46]

MS (ESI) m/z calculated for ($[M - Cl^-]^+$) 504.1039, found 504.0768.

Anal. Calcd for $C_{22}H_{17}ClN_2Pt$: C, 48.90; H, 3.17; N, 5.19. Found: C, 49.01; H, 3.24; N, 5.14.

Pt(F-mppy)(F-mppyH)Cl (1b). Reaction time: 24 h. Yield: 77.4%.

^{1}H NMR (500 MHz, Acetone d_6): δ 9.45 ("t", 1H, J_{Pt-H} = 19.2), 9.04 ("t", 1H, J_{Pt-H} = 21.7), 8.23 (td, 1H, J = 6.8, 3.0), 8.06 (d, 1H, J = 4.2), 7.84 (d, 1 H, J = 4.3), 7.78 (d, 1H, J = 4.3), 7.68 (d, 1H, J = 4.3), 7.53 (td, 1H, J = 6.9, 2.7), 7.12 (t, 2H, J = 8.8), 6.72 (td, 1H, J = 9.0, 2.2), 5.76 ("tdd", 1H, J_{Pt-H} = 26.5, J = 10.0, 2.4), 2.52 (s, 3H), 2.40 (s, 3H).

(31) Lee, J.-K.; Yoo, D. S.; Handy, E. S.; Rubner, M. F. *Appl. Phys. Lett.* **1996**, *69*(12), 1686.
(32) Tamayo, A. B.; Garon, S.; Sajoto, T.; Djurovich, P. I.; Tsyba, I. M.; Bau, R.; Thompson, M. E. *Inorg. Chem.* **2005**, *44*, 8723.
(33) Baldo, M. A.; Thompson, M. E.; Forrest, S. R. *Nature* **2000**, *403*, 750.
(34) Baldo, M. A.; O'Brien, D. F.; You, Y.; Shoustikov, A.; Sibley, S.; Thompson, M. E.; Forrest, S. E. *Nature* **1998**, *395*, 151.
(35) Slinker, J. D.; Rivnay, J.; Moskowitz, J. S.; Parker, J. B.; Bernhard, S.; Abruña, H. D.; Malliaras, G. G. *J. Mater. Chem.* **2007**, *17*, 2976.
(36) Wang, Y.; Li, B.; Liu, Y.; Zhang, L.; Zuo, Q.; Shi, L.; Su, Z. *Chem. Commun.* **2009**, 5868.
(37) Mills, A.; Lepre, A.; Theobald, B. R. C.; Slade, E.; Murrer, B. A. *Gold Bull.* **1998**, *31*(2), 68.
(38) Xu, W.; McDonaough, R. C., III; Langsdorf, B.; Demas, J. N.; DeGraff, B. A. *Anal. Chem.* **1994**, *66*, 4133.
(39) Di Censo, D.; Fantacci, S.; De Angelis, F.; Klein, C.; Evans, N.; Kalyanasundaram, K.; Bolink, H. J.; Gratzel, M.; Nazeeruddin, M. K. *Inorg. Chem.* **2008**, *47*, 980.
(40) Muller, P.; Schroder, B.; Parkinson, J. A.; Kratochwil, N. A.; Coxall, R. A.; Parkin, A.; Parsons, S.; Sadler, P. J. *Angew. Chem., Int. Ed.* **2003**, *42*, 335.
(41) Kaluderovic, G. N.; Kommera, H.; Schwieger, S.; Paethanom, A.; Kunze, M.; Schmidt, H.; Paschke, R.; Steinborn, D. *Dalton Trans.* **2009**, 10720.
(42) Kelland, L. *Nat. Rev. Cancer* **2007**, *7*, 573.
(43) McKeage, M. J.; Mistry, P.; Ward, J.; Boxall, F. E.; Loh, S.; O'Neill, C.; Ellis, P.; Kelland, L. R.; Morgan, S. E.; Murrer, B.; Santabarbara, P.; Harrap, K. R.; Judson, I. R. *Cancer Chemother. Pharmacol.* **1995**, *36*, 451. DNE.
(44) Periana, R. A.; Taube, D. J.; Gamble, S.; Taube, H.; Satoh, T.; Fujii, H. *Science* **1998**, *280*, 560.
(45) Aleman, J.; del Solarb, V.; Navarro-Ranninger, C. *Chem. Commun.* **2010**, *46*, 454.
(46) Niedermair, F.; Waich, K.; Kappaun, S.; Mayr, T.; Trimmel, G.; Mereiter, K.; Slugovc, C. *Inorg. Chim. Acta* **2007**, *360*, 2767.

^{13}C NMR (500 MHz, Acetone d_6): δ 164.91 (s), 164.68 (d, J = 29.3), 162.94 (s), 158.78 (s), 157.36 (s), 155.11 (d, J = 48.0), 151.19 (s), 145.46 (s), 140.63 (d, J = 50.8), 139.80 (s), 136.41 (d, J = 3.2), 135.64 (s), 135.06 (s), 132.83 (d, J = 8.6), 131.93 (d, J = 8.6), 127.96 (s), 126.20 (s), 125.83 (d, J = 9.4), 119.07 (s), 116.05 (d, J = 22.1), 115.36 (d, J = 22.1), 30.63 (s), 18.13 (s), 17.89 (s), 17.85 (s).

^{19}F NMR (300 MHz, Acetone d_6): δ −111.49 (s), −113.06 (d, J = 169.6).

MS (ESI) m/z calculated for ([M − Cl$^-$]$^+$) 568.1164, found 568.0874.

Pt(MeO-mppy)(MeO-mppyH)Cl (1c). Reaction time: 24 h. Yield: 81.4%.

^{1}H NMR (500 MHz, Acetone d_6): δ 9.44 ("t", 1H, J_{Pt-H} = 17.35), 9.03 ("t", 1H, J_{Pt-H} = 20.3), 8.23 (d, 2H, J = 4.8), 7.98 (d, 1H, J = 4.1), 7.76 (d, 1H, J = 4.4), 7.71 (d, 1H, J = 4.4), 7.58 (d, 1H, J = 4.2), 7.38 (d, 1H, J = 4.7), 6.89 (d, 2H, J = 4.6), 6.53 (dd, 1H, J = 4.4, 2.3), 5.59 ("td", 1H, J_{Pt-H} = 26.7, J = 2.4), 3.75 (s, 3H), 3.57 (s, 3H), 2.49 (s, 3H), 2.37 (s, 3H).

^{13}C NMR (500 MHz, Acetone d_6): δ 165.59 (s), 161.27 (s), 161.11 (s), 159.69 (s), 154. 92 (s), 150.90 (s), 144.46 (s), 140.35 (s), 139.92 (s), 138.07 (s), 134.41 (s), 133.45 (s), 131.95 (s), 131.40 (s), 127.56 (s), 125.25 (s), 118.19 (s), 116.47 (s), 113.85 (s), 108.97 (s), 55.50 (s), 55.04 (s), 18.07 (s), 17.78 (s).

MS (ESI) m/z calculated for ([M − Cl$^-$]$^+$) 592.1564, found 592.1384.

Pt(Ph-mppy)(Ph-mppyH)Cl (1d). Reaction time: 24 h. Yield: 88.5%.

^{1}H NMR (300 MHz, $CDCl_3$): δ 9.48 (s), 9.16 (s), 8.34 (d, J = 8.3), 8.23 (d, J = 8.3), 8.08 (d, J = 8.3), 8.01 (m), 7.72 (m), 7.66 (m), 7.63 (m), 7.61−7.28 (m), 7.22 (J = 1.8), 7.19 (J = 1.8), 7.04 (J = 8.0), 6.40 (J = 1.7), 4.61 (s), 2.48 (s), 2.42 (J = 2.7), 2.36 (s).

MS (ESI) m/z calculated for ([M − Cl$^-$]$^+$) 684.1978, found 684.1851.

Synthesis of Pt(ppy)$_2$Cl$_2$ Derivatives. The precursor bis-cyclometalated Pt^{IV} dichloride complexes were synthesized using a method similar to that reported by Mamtora et al.[47] The parent Pt^{II} pendant complex was reacted with iodobenzene dichloride in dichloromethane at room temperature. The precipitate was filtered and washed in dichloromethane for modest to good yields (16−72%). The bis-cyclometalated products can also be obtained by oxidation of (**1a**)−(**1d**) with hydrogen peroxide as reported by Newman et al.[47]

Pt(ppy)$_2$Cl$_2$ (2a). Pt(ppy)(ppyH)Cl (0.222 g, 0.411 mmol) was reacted with iodobenzene dichloride (0.113 g, 0.411 mmol) in 20 mL of dichloromethane for 24 h. A white solid precipitated and was collected by filtration and washed in dichloromethane (20 mL). Yield: 0.170 g (72.1%).

^{1}H NMR (500 MHz, DMSO d_6): δ 9.72 ("td", 2H, J_{Pt-H} = 14.3, J = 6.0), 8.49 (d, 2H, J = 7.9), 8.39 (ddd, 2H, J = 9.0, 7.8, 1.1), 7.97 (d, 2H, J = 7.9), 7.82 (td, 2H, J = 6.7, 1.2), 7.16 (t, 2H, J = 7.4), 6.98 (td, 2H, J = 7.6, 1.1), 5.94 ("td", 2H, J_{Pt-H} = 16.2, J = 7.9).

^{13}C NMR (500 MHz, DMSO d_6): 163.20 ("t", J_{Pt-C} = 28.1), 148.83 (s), 142.80 (s), 141.24 (s), 140.60 ("t", J_{Pt-C} = 14.6), 131.60 ("t", J_{Pt-C} = 21.1), 126.46 ("t", J_{Pt-C} = 15.8), 125.82 (m), 124.99 ("t", J_{Pt-C} = 13.8), 121.69 ("t", J_{Pt-C} = 15.7).

Anal. Calcd for $C_{22}H_{16}Cl_2N_2Pt$: C, 46.01; H, 2.81; N, 4.88. Found: C, 45.89; H, 2.89; N, 4.77.

Pt(F-mppy)$_2$Cl$_2$ (2b). Yield: 54.7%.

^{1}H NMR (500 MHz, DMSO d_6): δ 9.45 ("t", 2H, J_{Pt-H} = 14.0), 8.38 (d, 2H, J = 8.6), 8.26 (dd, 2H, J = 8.3, 1.1), 8.07 (dd, 2H, J = 8.7, 5.8), 7.07 (td, 2H, J = 8.9, 2.4), 5.65 ("tdd", 2H, J_{Pt-H} = 18.6, J = 8.5, 2.4), 3.37 (s).

^{13}C NMR (500 MHz, DMSO d_6): δ 160.70 (s), 159.63 (s), 147.65 (s), 142.89 (s), 141.99 (d, J = 6.4), 137.37 (d, J = 2.0), 135.19 (s), 127.77 (d, J = 9.1), 121.48 ("t", J_{Pt-C} = 16.4), 113.29 (d, J = 21.7), 112.99 (d, J = 23.1), 18.15 (s).

^{19}F NMR (300 MHz, DMSO d_6): δ −106.86 (dd, J = 14.0, 8.2).

Pt(MeO-mppy)$_2$Cl$_2$ (2c). Yield: 15.6%.

^{1}H NMR (500 MHz, DMSO d_6): δ 9.42 (t, 2H, J = 13.9), 8.25 (d, 2H, J = 8.3), 8.16 (dd, 2H, J = 8.6, 1.2), 7.88 (d, 2H, J = 8.7), 6.76 (dd, 2H, J = 8.7, 2.2), 5.30 ("td", 2H, J_{Pt-H} = 18.5, J = 2.3), 3.56 (s), 3.37 (s).

^{13}C NMR (500 MHz, DMSO d_6): δ 160.76 (t, J = 27.0), 160.14 (t, 2H, J = 26.5), 147.26 (s), 142.33 (s), 142.04 (s), 133.33 ("d", J = 13.9), 127.04 ("t", J_{Pt-C} = 18.0), 120.36 ("t", J_{Pt-C} = 17.4), 112.81 ("t", J_{Pt-C} = 17.1), 109.71 (s), 55.03 (s), 17.97 (s).

Pt(Ph-mppy)$_2$Cl$_2$ (2d). Yield: 34.8%.

^{1}H NMR (300 MHz, DMSO d_6): δ 9.60 ("t", 2H, J_{Pt-H} = 14.5), 8.43 (m, 2H), 8.28 (d, 2H, J = 8.7), 8.00 (d, 2H, J = 8.2), 7.45 (dd, 2H, J = 8.4, 1.2), 7.35 (m, 6H), 7.28 (m, 4H), 6.10 ("td", 2H, J_{Pt-H} = 17.4, J = 1.5), 2.58 (s, 6H).

^{13}C NMR (300 MHz, DMSO d_6): δ 161.00 ("t", J_{Pt-C} = 24.4), 148.49 (s), 143.04 (s), 142.81 (s), 141.83(s), 140.39 ("t", J_{Pt-C} = 14.0), 135.49 ("t", J_{Pt-C} = 14.4), 129.57 (s), 128.61 (s), 126.86 (s), 126.54 ("t", J_{Pt-C} = 15.4), 124.91 (s), 124.44 ("t", J_{Pt-C} = 17.4), 121.90 ("t", J_{Pt-C} = 15.4), 18.62 (s).

Synthesis of [Pt(ppy)$_2$(bpy)](PF$_6$)$_2$ Derivatives. All [Pt(ppy)$_2$(bpy)](PF$_6$)$_2$ derivatives were synthesized using similar conditions. The Pt^{IV} dichloride was heated with an excess of the N^N ligand in a non-reducing solvent system (acetonitrile/water, *tert*-butanol/water, or water) and chloride departure was assisted using Ag$^+$ or Tl$^+$ ion, when necessary, in a manner similar to that used by McDaniel et al.[48] The mixture was diluted with water and ammonium hexafluorophosphate was added to precipitate a solid which was then filtered. The solid was dried in vacuo at 100 °C for 24 h and the purified product obtained as crystals using acetonitrile/ethyl ether vapor diffusion. All reactions were performed in 40 mL sealed glass vials equipped with septa.

[Pt(ppy)$_2$(bpy)](PF$_6$)$_2$ (3a). A 40 mL reaction vial, equipped with a septum, was charged with Pt(ppy)$_2$Cl$_2$ (0.050 g, 87.1 μmol), 2,2′-bipyridine (0.081 g, 519.3 μmol), and a magnetic stirrer in 10 mL of 3:1 acetonitrile/water. The reaction was stirred for 48 h at 110 °C and then cooled. The reaction mixture was diluted to 20 mL with water, ammonium hexafluorophosphate (0.425 g, 2.61 mmol) was added, and the mixture diluted to 50 mL with water to precipitate a solid. The solid was filtered and dried overnight in a vacuum oven at 100 °C. Recrystallization by diffusion of ethyl ether into acetonitrile containing the complex was performed to arrive at the pure compound (**3a**) (0.041 g, 50%).

^{1}H NMR (500 MHz, Acetone d_6): δ 9.12 (d, 2H, J = 8.6), 8.65 (td, 4H, J = 7.9, 1.4), 8.47 (td, 2H, J = 7.8, 1.3), 8.32 (q, 2H, J = 6.1), 8.24 (m, 4H), 8.03 (ddd, 2H, J = 8.2, 5.5, 1.1), 7.57 (m, 4H), 7.33 (td, 2H, J = 7.6, 1.4), 6.43 ("td", 2H, J_{Pt-H} = 13.8, J = 8.2)

^{13}C NMR (500 MHz, Acetone d_6): δ 164.10 (s), 155.26 (s), 149.90 (s), 149.24 (s), 144.79 (s), 144.46 (s), 142.33 (s), 137.54 (s), 134.40 ("t", J_{Pt-C} = 18.6), 131.56 ("t", J_{Pt-C} = 8.2), 129.52 ("t", J_{Pt-C} = 14.7), 128.32 ("t", J_{Pt-C} = 13.9), 127.95 ("t", J_{Pt-C} = 13.9), 127.85 (s), 124.23 ("t", J_{Pt-C} = 16.8).

MS (ESI) m/z calculated for ([M − 2(PF$_6$)$^-$]$^{2+}$) 329.5825, found 329.5368.

Anal. Calcd for $C_{32}H_{24}F_{12}N_4P_2Pt$: C, 40.48; H, 2.55; N, 5.90. Found: C, 40.62; H, 2.78; N, 6.02.

[Pt(ppy)$_2$(dFbpy)](PF$_6$)$_2$ (3b). A 40 mL reaction vial, equipped with a septum, was charged with Pt(ppy)$_2$Cl$_2$ (0.088 g, 153.2 μmol), 5,5′-difluoro-2,2′-bipyridine (0.119 g, 619.8 μmol), silver^{I}

(47) (a) Mamtora, J.; Crosby, S. H.; Newman, C. P.; Clarkson, G. J.; Rourke, J. P. *Organometallics* **2008**, *27*, 5559. (b) Newman, C. P.; Casey-Green, K.; Clarkson, G. J.; Cave, G. W. V.; Errington, W.; Rourke, J. P. *Dalton Trans.* **2007**, 3170.

(48) McDaniel, N. D.; Coughlin, F. J.; Tinker, L. L.; Bernhard, S. *J. Am. Chem. Soc.* **2008**, *130*, 210.

trifluoromethanesulfonate (0.083 g, 323.3 μmol), and a magnetic stirrer in 8 mL of 3:1 *tert*-butanol/water. The reaction was stirred for 24 h at 60 °C and then cooled. The reaction mixture was filtered, diluted to 20 mL with water, ammonium hexafluorophosphate (0.667 g, 4.1 mmol) was added, and the mixture diluted to 50 mL with water to precipitate a solid. The solid was filtered and dried overnight in a vacuum oven at 100 °C. Recrystallization by diffusion of ethyl ether into acetonitrile containing the complex was performed to arrive at the pure compound (**3b**) (0.102 g, 68%).

^{1}H NMR (500 MHz, Acetone d_6): δ 9.18 (dd, 2H, J = 5.1, 4.2), 8.65 (m, 2H), 8.52 (ddd, 2H, J = 9.6, 8.3, 2.7), 8.48 (td, 2H, J = 7.9, 1.2), 8.32 ("td", 2H, J_{Pt-H} = 14.0, J = 6.1), 8.23 (dd, 2H, J = 7.7, 1), 8.18 (dd, 2H, J = 7.0), 7.57 (q, 4H, J = 7.4), 7.33 (td, 2H, J = 7.7, 1.3), 6.41 ("td", 2H, J_{Pt-H} = 14.1, J = 8.0).

^{13}C NMR (500 MHz, Acetone d_6): δ 163.16 (d, J = 262), 163.96 (s), 151.27 (d, J = 3.3), 149.53 (s), 144.83 (s), 142.49 (s), 139.54 (d, J = 32.8), 136.53 (s), 134.41 ("t", J_{Pt-C} = 19.3), 131.50 (d, J = 19.1), 130.00 (m), 129.77 (s), 129.67 ("t", J_{Pt-C} = 13.9), 128.46 ("t", J_{Pt-C} = 13.8), 127.92 ("t", J_{Pt-C} = 13.8), 124.36 ("t", J_{Pt-C} = 16.4).

^{19}F NMR (300 MHz, Acetone d_6): δ −115.17 (s).

MS (ESI) m/z calculated for ($[M - 2(PF_6)^-]^{2+}$) 347.5730, found 347.5255.

Anal. Calcd for $C_{32}H_{22}F_{14}N_4P_2Pt \cdot H_2O$: C, 38.30; H, 2.41; N, 5.58. Found: C, 38.28; H, 2.38; N, 5.52.

[Pt(ppy)$_2$(dMeObpy)](PF$_6$)$_2$ (3c). A 40 mL reaction vial, equipped with a septum, was charged with $Pt(ppy)_2Cl_2$ (0.048 g, 83.6 μmol), 4,4′-dimethoxy-2,2′-bipyridine (0.108 g, 499.5 μmol), and a magnetic stirrer in 6 mL of 3:1 acetonitrile/water. The reaction was stirred for 48 h at 110 °C and then cooled. The reaction mixture was diluted to 11 mL with water and washed in ethyl ether (3 × 10 mL). Ammonium hexafluorophosphate (0.380 g, 2.3 mmol) was added, and the mixture diluted to 50 mL with water to precipitate a solid. The solid was filtered and dried overnight in a vacuum oven at 100 °C. Recrystallization by diffusion of ethyl ether into acetonitrile containing the complex was performed to arrive at the pure compound (**3c**) (0.058 g, 71%).

^{1}H NMR (500 MHz, Acetone d_6): δ 8.65 (m, 2H), 8.59 (d, 2H, J = 2.6), 8.48 (ddd, 2H, J = 9.3, 8.0, 1.1), 8.23 (m, 4H), 8.0 (d, 2H, J = 6.5), 7.61 (ddd, 2H, J = 8.5, 5.9, 1.3), 7.53 (td, 2H, J = 7.7), 7.46 (dd, 2H, J = 6.7, 2.6), 7.3 (td, 2H, J = 7.7, 1.3), 6.40 ("td", 2H, J_{Pt-H} = 13.5, J = 7.8), 4.15 (s, 6H).

^{13}C NMR (500 MHz, Acetone d_6): δ 171.37 (s), 164.22 (s), 156.81 (s), 150.56 ("t", J_{Pt-C} = 9.0), 148.93 (s), 144.70 (s), 142.31 (s), 137.91 (s), 134.31 ("t", J_{Pt-C} = 18.4), 129.49 ("t", J_{Pt-C} = 14.4), 129.31 (s), 128.21 ("t", J_{Pt-C} = 13.1), 127.88 ("t", J_{Pt-C} = 14.4), 124.12 ("t", J_{Pt-C} = 16.4), 116.42 ("t", J_{Pt-C} = 8.15), 114.37 ("t", J_{Pt-C} = 5), 58.04 (s).

MS (ESI) m/z calculated for ($[M - 2(PF_6)^-]^{2+}$) 359.5930, found 359.5447.

Anal. Calcd for $C_{34}H_{28}F_{12}N_4O_2P_2Pt \cdot 3H_2O$: C, 38.39; H, 3.22; N, 5.27. Found: C, 38.39; H, 3.17; N, 5.24.

[Pt(F-mppy)$_2$(bpy)](PF$_6$)$_2$ (3d). A 40 mL reaction vial, equipped with a septum, was charged with $Pt(F\text{-}mppy)_2Cl_2$ (0.080 g, 125.4 μmol), 2,2′-bipyridine (0.039 g, 250.0 μmol), silver[I] trifluoromethanesulfonate (0.069 g, 268.8 μmol) and a magnetic stirrer in 6 mL acetonitrile. The reaction was stirred for 24 h at 70 °C and then cooled. The reaction mixture was filtered, diluted to 18 mL with water and washed in ethyl ether (3 × 20 mL). Ammonium hexafluorophosphate (0.610 g, 3.7 mmol) was added, and the mixture diluted to 50 mL with water to precipitate a solid. The solid was filtered and dried overnight in a vacuum oven at 100 °C. Recrystallization by diffusion of ethyl ether into acetonitrile containing the complex was performed to arrive at the pure compound (**3d**) (0.070 g, 63%).

^{1}H NMR (500 MHz, Acetone d_6): δ 9.06 (d, 2H, J = 8.3), 8.66 (td, 2H, J = 7.5, 1.7), 8.51 (m, 2H), 8.39 (ddd, 2H, J = 5.7, 6.6, 1.1), 8.31 (m, 4H), 8.01 (m, 4H), 7.37 (td, 2H, J = 8.8, 2.4), 6.14 ("tdd", 2H, J_{Pt-H} = 16.3, J = 8.2, 2.5), 2.22 (s, 6H).

^{13}C NMR (500 MHz, Acetone d_6): δ 160.14 (s), 155.34 (s), 150.25 (s), 148. 32 (s), 145.70 (t, J = 3.4), 144.48 (s), 139.09 (s), 138.99 (m), 138.02 (d, J = 7.7), 131.50 ("t", J_{Pt-C} = 8.3), 130.17 (d, J = 10.0), 127.97 ("t", J_{Pt-C} = 5.0), 123.77 ("t", J_{Pt-C} = 16.9), 116.96 (d, J = 23), 116.58 (d, J = 22.8), 114.02 (s), 18.40 (s).

^{19}F NMR (300 MHz, Acetone d_6): δ −105.12 (m).

MS (ESI) m/z calculated for ($[M - 2(PF_6)^-]^{2+}$) 361.5886, found 361.5665.

Anal. Calcd for $C_{34}H_{26}F_{14}N_4P_2Pt \cdot 2.5\ H_2O$: C, 38.57; H, 2.95; N, 5.29. Found: C, 38.53; H, 2.76; N, 5.30.

[Pt(F-mppy)$_2$(dFbpy)](PF$_6$)$_2$ (3e). A 40 mL reaction vial, equipped with a septum, was charged with $Pt(F\text{-}mppy)_2Cl_2$ (0.080 g, 125.4 μmol), 5,5′-difluoro-2,2′-bipyridine (0.144 g, 750.0 μmol), thallium[I] nitrate (0.180 g, 675.7 μmol), and a magnetic stirrer in 15 mL of water. The reaction was stirred for 96 h at 110 °C and then cooled. The reaction mixture was filtered, and ammonium hexafluorophosphate (0.300 g, 1.8 mmol) was added to precipitate a solid. The solid was filtered and dried overnight in a vacuum oven at 100 °C. Recrystallization by diffusion of ethyl ether into acetonitrile containing the complex was performed to arrive at the pure compound (**3e**) (0.024 g, 18%).

^{1}H NMR (500 MHz, Acetone d_6): δ 9.14 (dd, 2H, J = 9.4, 3.7), 8.53 (m, 4H), 8.30 (m, 6H), 8.09 ("t", 2H, J_{Pt-H} = 14.1), 7.38 (td, 2H, J = 8.9, 2.0), 6.11 ("tdd", 2H, J_{Pt-H} = 17.0, 8.5, 2.2), 2.23 (s, 6H).

^{13}NMR (500 MHz, Acetone d_6): δ 164.96 (s), 163.01 (d, J = 261), 162.92 (s), 160.36 (s), 151.35 (d, J = 3), 148.50 (s), 145.73 (s), 139.99 (d, J = 33), 139.13 (s), 136.84 (d, J = 7), 131.54 (d, J = 19), 130.28 (d, J = 9.0), 130.07 (d, J = 8.6), 123.94 ("t", J_{Pt-C} = 17.4), 117.12 (d, J = 23.0), 116.83 (d, J = 22.5), 18.38 (s).

^{19}F NMR (300 MHz, Acetone d_6): δ −104.94 (dd, J = 17.6, 5.8), −115.18 (s).

MS (ESI) m/z calculated for ($[M - 2(PF_6)^-]^{2+}$) 379.5793, found 379.5661.

Anal. Calcd for $C_{34}H_{24}F_{16}N_4P_2Pt \cdot H_2O$: C, 38.25; H, 2.45; N, 5.25. Found: C, 38.50; H, 2.55; N, 5.25.

[Pt(F-mppy)$_2$(dMeObpy)](PF$_6$)$_2$ (3f). A 40 mL reaction vial, equipped with a septum, was charged with $Pt(F\text{-}mppy)_2Cl_2$ (0.070 g, 109.7 μmol), 4,4′-dimethoxy-2,2′-bipyridine (0.047 g, 217.4 μmol), thallium[I] nitrate (0.073 g, 274.0 μmol), and a magnetic stirrer in 8 mL of 4:6 acetonitrile/water. The reaction was stirred for 96 h at 115 °C and then cooled. The reaction mixture was diluted to 16 mL with water, filtered, and washed in ethyl ether (3 × 20 mL). Ammonium hexafluorophosphate (0.540 g, 3.3 mmol) was added, and the mixture diluted to 50 mL with water to precipitate a solid. The solid was filtered and dried overnight in a vacuum oven at 100 °C. Recrystallization by diffusion of ethyl ether into acetonitrile containing the complex was performed to arrive at the pure compound (**3f**) (0.045 g, 38%).

^{1}H NMR (500 MHz, Acetone d_6): δ 8.57 (d, 2H, J = 2.2), 8.51 (d, 2H, J = 8.3), 8.30 (m, 4H), 8.10 ("q", 2H, J_{Pt-H} = 6.6), 8.02 ("t", 2H, J_{Pt-H} = 14.3), 7.45 (dd, 2H, J = 6.8, 2.4), 7.35 (td, 2H, J = 8.7, 2.0), 6.12 ("tdd", 2H, J_{Pt-H} = 15.7, 8.7, 2.0), 4.16 (s), 2.26 (s).

^{13}C NMR (500 MHz, Acetone d_6): δ 171.34 (s), 165.09 (s), 163.05 (s), 160.58 (s), 156.87 (s), 150.97 ("t", J_{Pt-C} = 10.7), 147.94 (s), 145.62 (s), 138.42 (s), 130.07 (d, J = 9.3), 123.69 ("t", J_{Pt-C} = 16.5), 116.90 (d, J = 23.0), 116.46 (s), 116.26 (m), 114.52 ("t", J_{Pt-C} = 5), 58.11 (s), 18.45 (s).

^{19}F NMR (300 MHz, Acetone d_6): δ −105.29 (m).

MS (ESI) m/z calculated for ($[M - 2(PF_6)^-]^{2+}$) 391.5992, found 391.5755.

Anal. Calcd for $C_{36}H_{30}F_{14}N_4O_2P_2Pt$: C, 40.27; H, 2.82; N, 5.22. Found: C, 40.18; H, 2.90; N, 5.22.

[Pt(MeO-mppy)$_2$(bpy)](PF$_6$)$_2$ (3g). A 40 mL reaction vial, equipped with a septum, was charged with $Pt(MeO\text{-}mppy)_2Cl_2$

(0.043 g, 65.0 μmol), 2,2′-bipyridine (0.060 g, 384.6 μmol), and a magnetic stirrer in 10 mL of 3:1 acetonitrile/water. The reaction was stirred for 48 h at 110 °C and then cooled. The reaction mixture was diluted to 20 mL with water, and ammonium hexafluorophosphate (0.450 g, 2.8 mmol) was added. The mixture was diluted to 50 mL with water to precipitate a solid. The solid was filtered and dried overnight in a vacuum oven at 100 °C. Recrystallization by diffusion of ethyl ether into acetonitrile containing the complex was performed to arrive at the pure compound (**3g**) (0.025 g, 37%).

^{1}H NMR (500 MHz, Acetone d_6): δ 9.05 (d, 2H, J = 8), 8.65 (td, 2H, J = 8.4, 1.3), 8.39 (m, 2H), 8.35 (d, 2H, J = 6), 8.22 (d, 2H, J = 8.5), 8.15 (d, 2H, J = 8.8), 8.02 (dd, 2H, J = 6.7), 7.92 ("t", 2H, J_{Pt-H} = 14.4), 7.13 (dd, 2H, J = 8.7, 2.3), 5.77 ("td", 2H, J_{Pt-H} = 16.1, 2.3), 3.75 (s, 6H), 2.19 (s, 6H).

^{13}C NMR (500 MHz, Acetone d_6): δ 162.98 (s), 161.68 (s), 155.35 (s), 150.04 ("t", J_{Pt-C} = 8.0), 147.69 (s), 145.23 (s), 144.25 (s), 138.52 (s), 137.32 (s), 131.36 ("t", J_{Pt-C} = 7.5), 129.55 ("t", J_{Pt-C} = 16.0), 127.79 ("t", J_{Pt-C} = 4.6), 122.61 ("t", J_{Pt-C} = 18), 115.90 ("t", J_{Pt-C} = 15), 113.25 (s), 56.02 (s), 18.23 (s).

MS (ESI) m/z calculated for ($[M - 2(PF_6)^-]^{2+}$) 373.6087, found 373.6040.

Anal. Calcd for $C_{36}H_{32}F_{12}N_4O_2P_2Pt \cdot H_2O$: C, 40.96; H, 3.25; N, 5.31. Found: C, 40.98; H, 3.29; N, 5.44.

[Pt(MeO-mppy)$_2$(dFbpy)](PF$_6$)$_2$ (3h). A 40 mL reaction vial, equipped with a septum, was charged with Pt(MeO-mppy)$_2$-Cl_2 (0.060 g, 90.6 μmol), 5,5′-difluoro-2,2′-bipyridine (0.104 g, 541.7 μmol), and a magnetic stirrer in 10 mL of 3:1 acetonitrile/water. The reaction was stirred for 48 h at 110 °C and then cooled. The reaction mixture was diluted to 20 mL with water, washed in ethyl ether (3 × 10 mL) and ammonium hexafluorophosphate (0.450 g, 2.8 mmol) was added. The mixture diluted to 50 mL with water to precipitate a solid. The solid was filtered and dried overnight in a vacuum oven at 100 °C. Recrystallization by diffusion of ethyl ether into acetonitrile containing the complex was performed to arrive at the pure compound (**3h**) (0.045 g, 47%).

^{1}H NMR (500 MHz, Acetone d_6): δ 9.13 (dd, 2H, J = 9.0, 4.0), 8.53 (dd, 2H, J = 9, 3), 8.38 (m, 2H), 8.22 (m, 2H), 8.14 (d, 2H, J = 8.9), 8.01 ("t", 2H, J_{Pt-H} = 14.0), 7.14 (dd, 2H, J = 9.0, 2.0), 5.74 ("td", 2H, J_{Pt-H} = 16.0, 2.0), 3.75 (s, 6H), 2.21 (s, 6H).

^{13}C NMR (500 MHz, Acetone d_6): δ 162.99 (d, J = 261), 162.91 (s), 161.53 (s), 151.35 (d, J = 3), 147.97 (s), 145.25 (s), 139.65 (d, J = 33.0), 137.46 (s), 137.38 (s), 134.62 (s), 131.32 (d, J = 19.0), 129.92 (m), 129.65 ("t", J_{Pt-C} = 16.0), 122.75 ("t", J_{Pt-C} = 18.0), 116.10 ("t", J_{Pt-C} = 15.0), 113.56 (s), 56.05 (s), 18.21 (s).

^{19}F NMR (300 MHz, Acetone d_6): δ −115.62 (s).

MS (ESI) m/z calculated for ($[M - 2(PF_6)^-]^{2+}$) 391.5992, found 391.6077.

Anal. Calcd for $C_{36}H_{30}F_{14}N_4O_2P_2Pt \cdot H_2O$: C, 39.61; H, 2.95; N, 5.13. Found: C, 39.79; H, 3.18; N, 5.12.

[Pt(MeO-mppy)$_2$(dMeObpy)](PF$_6$)$_2$ (3i). A 40 mL reaction vial, equipped with a septum, was charged with Pt(MeO-mppy)$_2$$Cl_2$ (0.060 g, 90.6 μmol), 4,4′-dimethoxy-2,2′-bipyridine (0.118 g, 545.8 μmol), and a magnetic stirrer in 10 mL of 3:1 acetonitrile/water. The reaction was stirred for 48 h at 110 °C and then cooled. The reaction mixture was diluted to 20 mL with water, and ammonium hexafluorophosphate (0.450 g, 2.8 mmol) was added. The mixture diluted to 50 mL with water to precipitate a solid. The solid was filtered and dried overnight in a vacuum oven at 100 °C. Recrystallization by diffusion of ethyl ether into acetonitrile containing the complex was performed to arrive at the pure compound (**3i**) (0.023 g, 23%).

^{1}H NMR (500 MHz, Acetone d_6): δ 8.56 (d, 2H, J = 2.5), 8.39 (m, 2H), 8.23 (d, 2H, J = 8.4), 8.13 (d, 2H, J = 9.0), 8.05 ("q", 2H, J_{Pt-H} = 6.5), 7.93 ("t", 2H, J_{Pt-H} = 14.0), 7.46 (dd, 2H, J = 6.6, 2.6), 7.11 (dd, 2H, J = 8.8, 2.2), 5.74 ("td", 2H, J_{Pt-H} = 15.9, 2.4), 4.16 (s, 6H), 3.73 (s, 6H), 2.24 (s, 3H).

^{13}C NMR (500 MHz, Acetone d_6): δ 171.20 (s), 162.96 ("t," J_{Pt-C} = 24.0), 161.80 (s), 156.88 (s), 150.79 ("t", J_{Pt-C} = 10.0), 147.33 (s), 145.15 (s), 138.88 (s), 137.26 (s), 134.50 (s), 129.46 ("t", J_{Pt-C} = 16.0), 122.55 (s), 116.18 ("t", J_{Pt-C} = 9.0), 115.84 ("t", J_{Pt-C} = 16.0), 114.32 ("t", J_{Pt-C} = 5.0), 113.16 (s), 58.03 (s), 55.99 (s), 18.28 (s).

MS (ESI) m/z calculated for ($[M - 2(PF_6)^-]^{2+}$) 403.6192, found 403.6086.

Anal. Calcd for $C_{38}H_{36}F_{12}N_4O_4P_2Pt \cdot H_2O$: C, 39.63; H, 3.68; N, 5.12. Found: C, 39.06; H, 3.65; N, 5.26.

[Pt(Ph-mppy)$_2$(bpy)](PF$_6$)$_2$ (3j). A 40 mL reaction vial, equipped with a septum, was charged with Pt(Ph-mppy)$_2$$Cl_2$ (0.050 g, 66.3 μmol), 2,2′-bipyridine (0.062 g, 394.7 μmol), and a magnetic stirrer in 10 mL of 3:1 acetonitrile/water. The reaction was stirred for 48 h at 110 °C and then cooled. The reaction mixture was diluted to 20 mL with water and ammonium hexafluorophosphate (0.425 g, 2.6 mmol) was added. The mixture diluted to 50 mL with water to precipitate a solid. The solid was filtered and dried overnight in a vacuum oven at 100 °C. Recrystallization by diffusion of ethyl ether into acetonitrile containing the complex was performed to arrive at the pure compound (**3j**) (0.016 g, 21%).

^{1}H NMR (300 MHz, Acetonitrile d_3): δ 8.77 (d, 2H, J = 8.2), 8.47 (td, 2H, J = 8.0, 1.5), 8.26 (m, 2H), 8.14 (dd, 2H, J = 0.9, 0.8), 8.12 (m, 2H), 8.03 (d, 2H, J = 8.2), 7.82 (d, 1H, J = 1.3), 7.80 (m, 2H), 7.76 (d, 1H, J = 1.7), 7.53 ("tt", 2H, J Pt−H = 14.5, J = 0.9), 7.43 (m, 10H), 6.36 ("td", 2H, J Pt−H = 14.5, J = 1.7), 2.18 (s, 6H).

^{13}C NMR (300 MHz, Acetonitrile d_3): δ 161.95 (s), 155.10 (s), 150.41 ("t", J_{Pt-C} = 8.1), 148.30 (s), 145.94 (s), 145.26 (s),144.05 (s), 141.29 (s), 139.86 (s), 138.93 (s), 137.36 (s), 131.21 ("t", J_{Pt-C} = 8.3), 130.14 (s), 129.68 (s), 128.41 ("t", J_{Pt-C} = 14.2), 127.96 (m), 127.35 ("t", J_{Pt-C} = 15.8), 123.76 (s), 17.59 (s).

MS (ESI) m/z calculated for ($[M - 2(PF_6)^-]^{2+}$) 419.6294, found 419.6114.

Anal. Calcd for $C_{46}H_{36}F_{12}N_4P_2Pt \cdot 2H_2O$: C, 47.39; H, 3.46; N, 4.81. Found: C, 47.57; H, 3.37; N, 4.98.

[Pt(Ph-mppy)$_2$(dMeObpy)](PF$_6$)$_2$ (3k). A 40 mL reaction vial, equipped with a septum, was charged with Pt(Ph-mppy)$_2$$Cl_2$ (0.100 g, 132.6 μmol), 4,4′-dimethoxy-2,2′-bipyridine (0.175 g, 809.4 μmol), and a magnetic stirrer in 14 mL of 3:1 acetonitrile/water. The reaction was stirred for 48 h at 110 °C and then cooled. The reaction mixture was diluted to 20 mL with water, washed with ethyl ether (3 × 20 mL), and ammonium hexafluorophosphate (0.680 g, 4.2 mmol) was added. The mixture diluted to 50 mL with water to precipitate a solid, which was filtered and dried overnight in a vacuum oven at 100 °C. Recrystallization by diffusion of ethyl ether into acetonitrile containing the complex was performed to arrive at the pure compound (**3k**) (0.026 g, 17%).

^{1}H NMR (300 MHz, Acetone d_6): δ 8.64 (d, 2H, J = 2.6), 8.58 (m, 2H), 8.34 (d, 2H, J = 8.6), 8.17 (m, 6H), 7.79 (dd, 2H, J = 8.3, 1.5), 7.42 (m, 12H), 6.55 (d, 2H, J = 1.5), 4.18 (s, 6H), 2.30 (s, 6H).

^{13}C NMR (300 MHz, Acetone d_6): δ 170.38 (s), 160.62 (s), 156.18 (s), 149.94 (t, J = 9.3), 147.34 (s), 144.94 (s), 144.41 (s), 140.44 (s), 138.99 (s), 137.90 (s), 137.12 (s), 129.04 (s), 128.53 (s), 127.32 (t, J = 13.7), 126.89 (s), 126.82 (s), 126.38 (t, J = 15.4), 122.68 (t, J = 17.3), 115.50 (t, J = 8.5), 113.45 (t, J = 5.0), 57.17 (s), 17.54 (s).

MS (ESI) m/z calculated for ($[M - 2(PF_6)^-]^{2+}$) 449.6400, found 449.6415.

Anal. Calcd for $C_{48}H_{40}F_{12}N_4O_2P_2Pt \cdot 3H_2O$: C, 46.35; H, 3.73; N, 4.50. Found: C, 45.95; H, 3.51; N, 4.64.

Spectroscopic and Spectrometric Determination. ^{1}H and ^{13}C NMR spectra were recorded on either a Bruker Avance-300 or a Bruker BioSpin Avance-500 MHz Spectrometer at room temperature. ^{19}F NMR spectra were recorded on a Varian-Mercury-VX 300 MHz Spectrometer. Mass Spectra (MS) were obtained using a Micromass Q-TOF II hybrid MS engine.

Scheme 1. Generalized Procedure for the Synthesis of Heteroleptic Pt^{IV} Complexes $[Pt(C^N)_2(N^N)](PF_6)_2$[a]

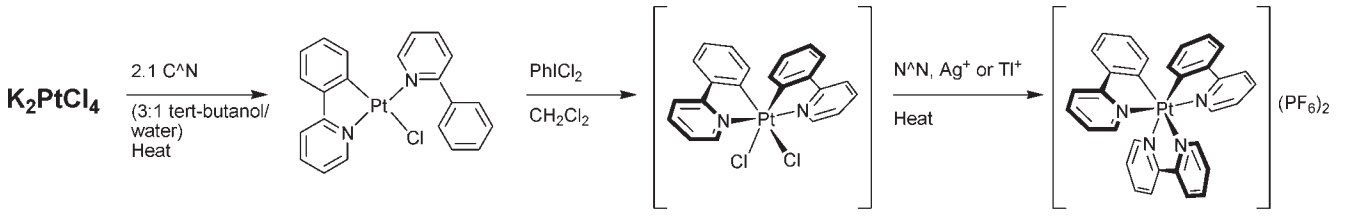

(1a) Pt(ppy)(ppyH)Cl
(1b) Pt(F-mppy)(F-mppyH)Cl
(1c) Pt(MeO-mppy)(MeO-mppyH)Cl
(1d) Pt(Ph-mppy)(Ph-mppyH)Cl

(2a) $Pt(ppy)_2Cl_2$
(2b) $Pt(F\text{-}mppy)_2Cl_2$
(2c) $Pt(MeO\text{-}mppy)_2Cl_2$
(2d) $Pt(Ph\text{-}mppy)_2Cl_2$

(3a) $[Pt(ppy)_2(bpy)](PF_6)_2$
(3b) $[Pt(ppy)_2(dFbpy)](PF_6)_2$
(3c) $[Pt(ppy)_2(dMeObpy)](PF_6)_2$
(3d) $[Pt(F\text{-}mppy)_2(bpy)](PF_6)_2$
(3e) $[Pt(F\text{-}mppy)_2(dFbpy)](PF_6)_2$
(3f) $[Pt(F\text{-}mppy)_2(dMeObpy)](PF_6)_2$
(3g) $[Pt(MeO\text{-}mppy)_2(bpy)](PF_6)_2$
(3h) $[Pt(MeO\text{-}mppy)_2(dFbpy)](PF_6)_2$
(3i) $[Pt(MeO\text{-}mppy)_2(dMeObpy)](PF_6)_2$
(3j) $[Pt(Ph\text{-}mppy)_2(bpy)](PF_6)_2$
(3k) $[Pt(Ph\text{-}mppy)_2(dMeObpy)](PF_6)_2$

[a] Modification of substituents on the ligands produced a family of 11 derivatives (**3a**)−(**3k**).

Table 1. Initial Set of Cyclometalating and Diimine Ligands

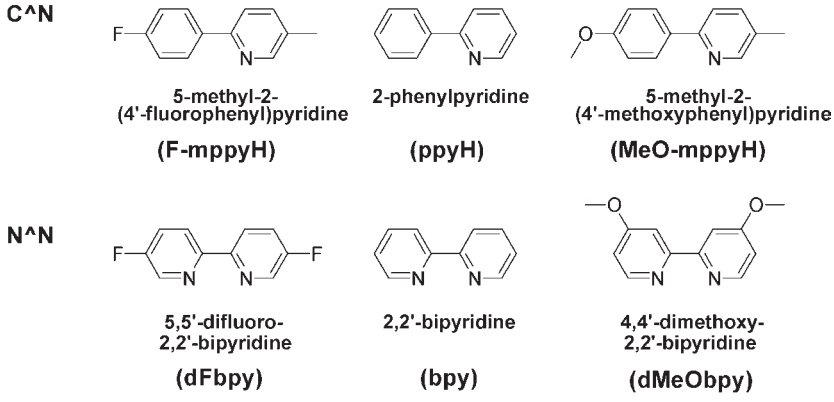

Photophysical Characterization. Photoluminescence measurements were performed at room temperature using 15 μM solutions in acetonitrile using a capped quartz cuvette (1.0 cm). These solutions were degassed using bubbling Argon for 10 min prior to each measurement. UV−vis absorption spectra were measured using either a Hewlett-Packard 8453 diode-array spectrophotometer or a Varian Cary 50 UV−vis spectrophotometer. Photoluminescence emission spectra were measured on a Jobin-Yvon Fluorolog-3 spectrophotometer equipped with dual monochromators and a Hamamatsu-928 photomultiplier tube (PMT) at right angle geometry. The emission spectra were recorded at an excitation wavelength of 317 nm and were corrected according to the calibration factors of the instrument. Photoluminescent quantum yields (Φ_{em}) were measured against a ruthenium^{II} tris(2,2′-bipyridine) hexafluorophosphate standard using the equation $\Phi_s = \Phi_r (I_s/I_r)(A_r/A_s)(\delta_s/\delta_r)$, where Φ_s is the quantum yield for the sample, I_s and I_r represent the points of maximum intensity in the corrected emission spectra of the sample and reference, A_s and A_r are the absorbance of the sample and the reference at the excitation wavelength, and δ_s and δ_r are the correction factors for sample and the reference for the heightened sensitivity of the detector to longer wavelengths. Φ_r is the quantum yield of the reference which is 6.2%.[49] Excited-state lifetimes (τ) were measured with the emission monochromator and PMT detector of the Jobin-Yvon spectrometer. The samples were excited at 337 nm using a Stanford Research Systems NL 100 N_2 laser (3.5 ns pulse). The emission decay was recorded using a Tektronix TDS 3032B digital phosphor oscilloscope.

Electrochemical Analyses. Electrochemical potentials were determined using a CH Instruments Model 600C Series Electrochemical Analyzer/Workstation with a potential sweep rate of 100 mV/s. Employed were a 1 mm^2 platinum working electrode, a platinum coil counter electrode, and a silver wire pseudo-reference electrode. Ferrocene (Aldrich) was used as an internal standard referenced against SCE as 0.371 V. Solutions of the complexes were prepared at ~400 μM and tetra-*n*-butylammonium hexafluorophosphate (Fluka, electrochemical grade) served as the supporting electrolyte at a concentration of 0.1 M. The solutions were degassed for 5 min with bubbling N_2 prior to each measurement.

Computational Studies. Hybrid density functional theory (DFT) calculations (B3LYP/LANL2DZ) were performed using the Gaussian 03 suite.[50] Default thresholds for gradient convergence were used; however, the threshold for wave function

(49) Caspar, J. V.; Meyer, T. J. *J. Am. Chem. Soc.* **1983**, *105*, 5583.

(50) Frisch, M. J.; et al. *Gaussian 03*, revision C.02; Gaussian, Inc.: Wallingford, CT, 2004.

convergence was relaxed to account for the presence of a heavy metal (CONVER = 7). All geometric optimizations were performed without point group constraints. For each metal complex, time-dependent DFT (TD-DFT) calculations were performed at the optimized ground-state geometry calculating the energy, oscillator strength, and rotory strength for each of the 200 lowest singlet excitations. Solvent effects (in acetonitrile) were taken into account by using the conductor polarizable continuum model (C-PCM, acetonitrile) in Gaussian 03. The lowest 10 triplet excitations were also obtained by using restricted B3LYP calculations at the optimized ground-state geometry. Calculation of UV−vis spectra was accomplished using GaussSum 2.0. Electronic transitions were expanded as Gaussian curves, with a fwhm (full width at half-maximum) for each peak set to 0.31 eV.

Results and Discussion

Synthetic Methods. At the onset, nine novel Pt^{IV} complexes were synthesized. The procedure used to obtain the complexes includes three steps, as seen below in Scheme 1. The first two steps include adaptations from the work of Neidermair et al.[46] and Mamtora et al.[47] utilizing Pt^{II} pendant complexes to obtain the bis-cyclometalated Pt^{IV} dichloride intermediates. Oxidation is accomplished by the reaction of the Pt^{II} pendant complex with a hypervalent iodide reagent in dichloromethane or via hydrogen peroxide in acetone. The final step is a modification of the procedure used by McDaniel[48] et al. to substitute the N^N ligand for the chlorides and arrive at the target complexes.

A combination of six different C^N and N^N ligands was chosen initially (Table 1). The choice of ligands was influenced by the desire to methodically investigate the effects of structural modification on the excited-state properties of the molecule and elucidate the degree of chemical tunability that could be attained. Electron-releasing groups on the ligand have been shown to significantly destabilize orbital energies, whereas electron-withdrawing groups demonstrate the opposite effect.[2] Therefore in addition to the parent ligands, 2-phenylpyridine (ppyH) and 2,2′-bipyridine (bpy), the methoxylated and fluorinated derivatives 5-methyl-2-(4-methoxyphenyl)-pyridine (MeO-mppyH), 4,4′-dimethoxy-2,2′-bipyridine (dMeObpy), 5-methyl-2-(4-fluorophenyl)-pyridine (F-mppyH), and 5,5′-difluoro-2,2′-bipyridine (dFbpy) were employed to study structure−property relations.

Upon characterizing the nine complexes mentioned above, the library was expanded by synthesizing two more complexes utilizing the C^N ligand 5-methyl-2-(biphen-4-yl)-pyridine (Ph-mppyH) and the N^N ligands bpy and dMeObpy.

Photophysical Characterization. Several interesting trends were observed in the photoluminescent characterization of the initial nine complex library. The complexes containing the ppy and F-mppy ligands exhibited blue, structured, steady-state luminescence, while the MeO-mppy derivatives were non-emissive in acetonitrile at room temperature (Figure 1). Emission maxima were significantly blue-shifted compared to the Ir^{III} analogues (482 nm for $[Pt(ppy)_2(bpy)](PF_6)_2$ versus 582 nm for $[Ir(ppy)_2(bpy)](PF_6)$[7]) and changed only marginally (~3 nm) upon variation of the N^N ligand, showing a sole dependence on the C^N ligand. The absorption and excitation spectra of $[Pt(ppy)_2(bpy)](PF_6)_2$ were identical indicating that emission was not due to an impurity (Black line,

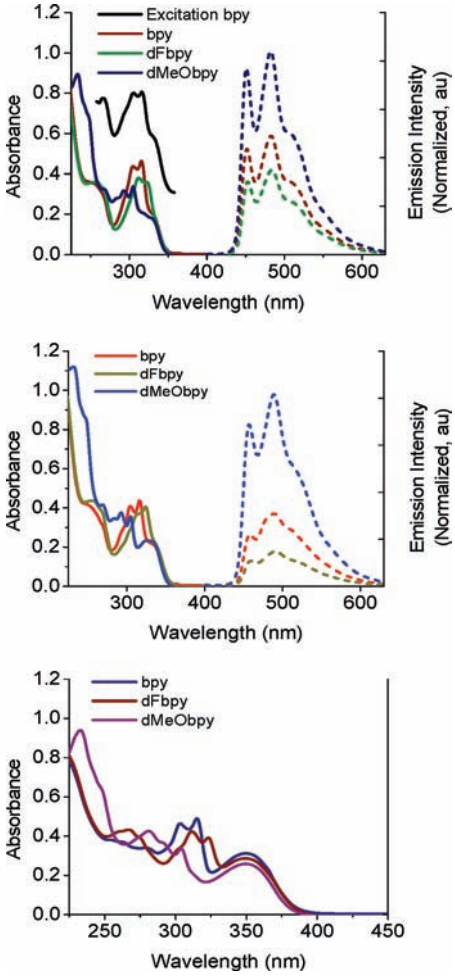

Figure 1. Excitation (black line), UV-absorption (solid line), and emission (dashed line) profiles of the $[Pt(ppy)_2(N^N)](PF_6)_2$ (top) and $[Pt(F\text{-}mppy)_2(N^N)](PF_6)_2$ series (middle), and UV-absorption of the $[Pt(MeO\text{-}mppy)_2(N^N)](PF_6)_2$ series (bottom). Two primary transitions are seen via UV−vis spectroscopy. The structured luminescence profiles and independence of emission maxima from the N^N ligand indicate a ^{3}LC emissive state on the C^N ligand. All spectra were measured in a 1 cm quartz cuvette using 15 μM solutions of the complex in acetonitrile, bubbling with N_2 for 10 min prior to the measurement. Emission profiles were obtained with an excitation wavelength of 317 nm.

Figure 1). Solvatochromic studies of $[Pt(ppy)_2(bpy)](PF_6)_2$ and $[Pt(ppy)_2(dMeObpy)](PF_6)_2$ showed no shift of emission maxima nor any change in the shape of the emission profiles in a range of solvents including tetrahydrofuran, methanol, *N*,*N*′-dimethylformamide, and chloroform in addition to acetonitrile. Therefore it can be concluded that the emissive state is primarily ligand centered (LC) arising from a $\pi-\pi^*$ transition on the C^N ligand.

Excited-state lifetimes of the complexes were found to be on the order of microseconds, ranging from 1.08 to 14.72 μs, and the quantum yields fell between 0.05% to 1.09% (Table 2). Longer excited-state lifetimes and higher quantum yields were observed for the ppy series than the F-mppy series, and a strong dependence on the N^N ligand was seen for both quantities in the order of dMeObpy > bpy > dFbpy. Furthermore, under an oxygen-saturated atmosphere, the lifetime of $[Pt(ppy)_2(bpy)](PF_6)_2$ decreased from 8.69 to 1.64 μs indicating a triplet emissive state and thus phosphorescence. Oxygen quenching studies showed that the six complexes exhibit similar sensitivity to oxygen;

Table 2. Photophysical Data for the Initial Library of Bis-Cyclometalated Pt^{IV} Complexes and Other Reference Complexes

complex	absorption[a] λ_{max}(nm)	emission[b] λ_{max}(nm)	$k_{nr}(10^3 s^{-1})$	$T^b(\mu s)$	Φ^c (%)	$K_{SV}[O_2]^b(mbar^{-1})$
(3a) $[Pt(ppy)_2(bpy)](PF_6)_2$	316 (3.08), 332 (sh)	452, 482, 511 (sh)	11.7	8.69 ± 0.06	0.29 ± 0.01	0.024 ± 0.001
(3b) $[Pt(ppy)_2(dFbpy)](PF6)$	323 (2.39), 332 (sh)	452, 484, 511(sh)	16.8	6.22 ± 0.05	0.27 ± 0.01	0.020 ± 0.001
(3c) $[Pt(ppy)_2(dMeObpy)](PF_6)_2$	305 (2.25), 332 (sh)	451, 482, 511 (sh)	7.35	14.72 ± 0.05	1.09 ± 0.05	0.037 ± 0.002
(3d) $[Pt(F\text{-}mppy)_2(bpy)](PF6)_2$	316 (2.91), 336 (sh)	457, 488, 520 (sh)	39.3	2.71 ± 0.07	0.09 ± 0.01	0.014 ± 0.001
(3e) $[Pt(F\text{-}mppy)_2(dFbpy)](PF_6)_2$	324 (2.70), 336 (sh)	460, 491, 520 (sh)	91.7	1.08 ± 0.07	0.05 ± 0.01	0.008 ± 0.001
(3f) $[Pt(F\text{-}mppy)_2(dMeOBpy)](PF6)_2$	305 (2.37), 336 (sh)	457, 489, 520 (sh)	13.1	8.28 ± 0.05	0.48 ± 0.02	0.026 ± 0.001
(3 g) $[Pt(MeO\text{-}mppy)_2(bpy)](PF_6)_2$	315 (3.27), 350 (2.08)					
(3 h) $[Pt(MeO\text{-}mppy)_2(dFbpy)](PF_6)_2$	323 (2.61), 349 (1.91)					
(3i)$[Pt(MeO\text{-}mppy)_2(dMeObpy)](PF_6)_2$	304 (2.25), 350 (1.72)					
$[Ru(bpy)_3](PF_6)_2$		608[d]	1000[d]	0.94[d]	6.20[d]	0.024 ± 0.001
$[Ir(ppy)_2(bpy)](PF_6)$		585[d]	2850[d]	0.33[d]	6.22[d]	0.026 ± 0.001
PtOEP		646[e]	12.5[e]	50[e]	37.5[e]	1.253 ± 0.055

[a] Absorption data were measured in acetonitrile solution at room temperature. Molar extinction coefficients (ε) in 10^4 M^{-1} cm^{-1} are listed in parentheses. [b] Emission spectra and excited-state lifetimes were measured in acetonitrile solution at room temperature after bubbling with argon for 10 min.; lifetimes were measured with a N_2 laser (3.5 ns pulse). [c] Quantum yields were calculated using $[Ru(bpy)_3](PF_6)_2$ as the reference standard.[49] [d] Ref 7. [e] Ref 51.

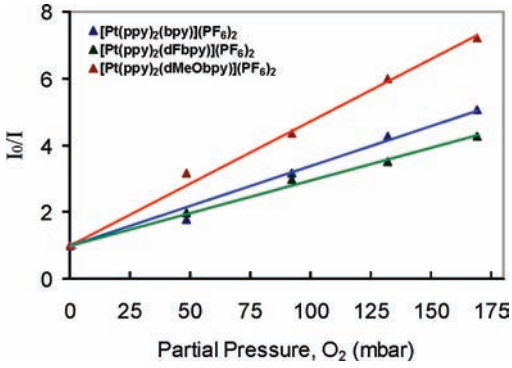

Figure 2. Stern−Volmer plot of $[Pt(ppy)_2(N^{\wedge}N)](PF_6)_2$ derivatives. Measurements were taken in a 1 cm quartz cuvette using 15 μM solutions of the complex in acetonitrile, bubbling with Argon/Oxygen mixtures for 10 min prior to the measurement with an excitation wavelength of 317 nm.

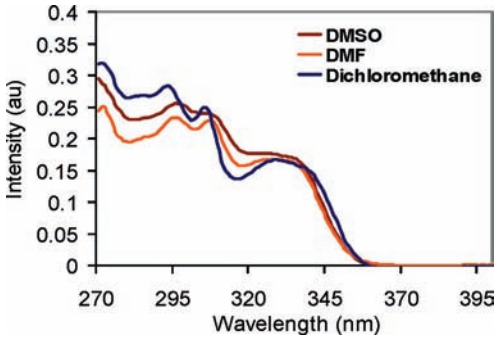

Figure 3. Modest solvatochromic effect is observed for the absorption of $[Pt(F\text{-}mppy)_2(dMeObpy)](PF_6)_2$. In non-polar solvents, a large degree of separation is seen between the ^{1}LLCT and ^{1}LC states; however, as solvent polarity is increased the ^{1}LLCT band is lowered in energy and the separation decreases.

Stern−Volmer constants were on the order of 0.01 to 0.04 $mbar^{-1}$. A Stern−Volmer plot of the $[Pt(ppy)_2(N^{\wedge}N)](PF_6)_2$ series is shown in Figure 2.

Characterization of the nine complexes by absorption spectrophotometry showed two primary transitions: a sharper, structured band at higher energies and a broad, unstructured band at lower energies (Figure 1). The unstructured band was partially or mostly obscured by the structured band in the ppy and F-mppy complexes, but was distinctly separate in the spectra of the MeO-mppy complexes. Across a $C^{\wedge}N$ series, the structured band was shifted to higher energies as the donor strength of the $N^{\wedge}N$ ligand increased, while the unstructured band was unaffected by the change. Additionally, when the $C^{\wedge}N$ ligand was varied across a $N^{\wedge}N$ series, the position of the unstructured transition was shifted, while no effect upon the structured transition was observed.

The nature of these absorption transitions was further probed in solvents of differing polarity. For $[Pt(ppy)_2(bpy)](PF_6)_2$ and $[Pt(F\text{-}mppy)_2(dMeObpy)](PF_6)_2$, as solvent polarity increased, the structured transition was red-shifted with regards to the unstructured transition, and the separation between the two bands therefore decreased. Figure 3 shows the solvatochromic effect upon the absorption profile of $[Pt(F\text{-}mppy)_2(dMeObpy)](PF_6)_2$. On the basis of these data, it is reasonable to assign the structured band to a charge-separated state, either a ligand to ligand charge transfer (LLCT) from the $C^{\wedge}N$ ligand to the $N^{\wedge}N$ ligand or a mixed ligand−metal to ligand charge transfer depending upon the degree to which the metal orbitals are involved. The unstructured band is assigned to a ligand-centered (LC) transition on the $C^{\wedge}N$ ligand.

Electrochemical Properties. Characterization of the Pt^{IV} complexes by cyclic voltammetry showed contrasting and unique electrochemical behavior compared to other analogous heteroleptic cyclometalated transition metal complexes,[4,5,12,52] most of which exhibit one-electron, metal-centered oxidation and one-electron, ligand-centered reduction. Despite the difference in ligand structure, all Pt^{IV} complexes studied showed comparable redox behavior (Table 3). While oxidation to Pt^{V} was not observable in the electrochemical window of the solvent, each complex exhibited an irreversible reduction wave around −1.0 V versus SCE that remained irreversible at scan rates as high as 10 V/s for complex (**3a**), which was followed by a quasi-reversible reduction near −1.96 V versus SCE.

To understand this redox behavior it is important to note that species of Pt^{III} are notoriously unstable because of the occupation of a high energy antibonding e_g*-type orbital. Additionally, neutral bis-cyclometalled Pt^{II} complexes such as $Pt(ppy)_2$ also exhibit quasi-reversible reduction at ∼ −1.96 V versus SCE.[4,53] Therefore the

(51) (a) Bansal, A. K.; Holzer, W.; Penzkofer, A.; Tsuboi, T. *Chem. Phys.* **2006**, *330*, 118. (b) Dienel, T.; Prohel, H.; Fritz, T.; Leo, K. *J. Lumin.* **2004**, *110*, 253.

Table 3. Electrochemical Data for the Initial Library of Bis-Cyclometalated Pt^{IV} Complexes[a]

complex	$E_{pc}Pt^{IV}/Pt^{II}$ (V vs SCE)	$E_{1/2}Pt^{II}(ppy)_2$ (V vs SCE)	ΔE_p (mV)
(3a) $[Pt(ppy)_2(bpy)](PF_6)_2$	−1.043	−1.965	84
(3b) $[Pt(ppy)_2(dFbpy)](PF_6)_2$	−0.986	−1.964	75
(3c) $[Pt(ppy)_2(dMeObpy)](PF_6)_2$	−1.122	−1.975	119
(3d) $[Pt(F\text{-}mppy)_2(bpy)](PF_6)_2$	−0.982	−1.970	99
(3e) $[Pt(F\text{-}mppy)_2(dFbpy)](PF_6)_2$	−0.933	−1.973	79
(3f) $[Pt(F\text{-}mppy)_2(dMeObpy)](PF_6)_2$	−1.063	−1.964	102
(3 g) $[Pt(MeO\text{-}mppy)_2(bpy)](PF_6)_2$	−1.081	−2.082	145
(3 h) $[Pt(MeO\text{-}mppy)_2(dFbpy)](PF_6)_2$	−1.017	−2.100	133
(3i) $[Pt(MeO\text{-}mppy)_2(dMeObpy)](PF_6)_2$	−1.155	n/a	n/a

[a] Measurements were taken of ~400 μM solutions of the complex in acetonitrile after bubbling with N_2 for five minutes. Tetrabutylammonium hexafluorophosphate (TBAH) was used as the supporting electrolyte at a concentration of 0.1M. The experimental apparatus included a 1 mm^2 platinum working electrode, a platinum coil counter electrode, and a silver wire pseudo-reference electrode; ferrocene was used as an internal standard referenced against SCE at 0.371 V.

electrochemical data are most likely explained by the reduction of the Pt^{IV} to Pt^{II} (either by way of disproportionation of the transient Pt^{III} species or two subsequent one-electron transfers to Pt^{IV}) observed at ~ −1 V versus SCE. This process triggers the fast loss of the N^N ligand to form the bis-cyclometaled Pt^{II} complex, the reduction of which is seen at ~ −1.96 V versus SCE (Figure 4). The formation of a Pt^{III} complex is not altogether impossible, as a few stable examples, most notably dimers, are recorded in the literature.[54,55] However, the evidence argues more strongly for the formation of the Pt^{II} complex. This is in agreement with the previously studied redox behavior of octahedral Pt^{IV} amine-halide compounds whereby two coordination sites are vacated and a square planar geometry is adopted to accommodate the resulting d^8 Pt^{II} center. This process is commonly seen in the activation of Pt^{IV} anticancer agents.[56−58] Furthermore, Sargeson et al. have reported on $[Pt(tame)_2]^{4+}$, a complex with a related structure, that undergoes the same conformational change upon reduction.[59]

It should also be noted that the potential required for the reduction of the Pt^{IV} center within a particular C^N series increases as a function of the donor ability of the N^N ligand in the order of dFbpy < bpy < dMeObpy. This variation corresponds to an increasing bond strength between the N^N ligand and Pt and correlates with the raised energy of the e_g* orbital. A similar trend was also observed for luminescence intensity and quantum yield indicating that the non-emissive ^{3}MC state is rendered less accessible for thermal population.[1]

Computational Investigation. Geometry optimizations for both the singlet and the triplet states were performed on the nine Pt^{IV} compounds from the initial library using DFT calculations. The use of B3LYP/LANL2DZ for

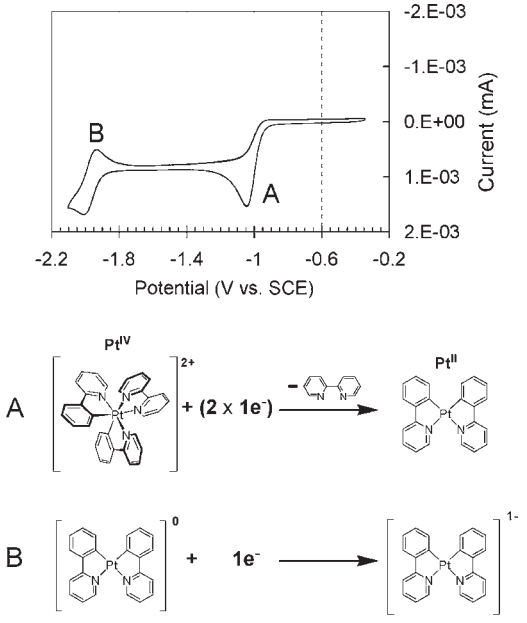

Figure 4. Cyclic voltammogram (top) of $[Pt(ppy)_2(bpy)](PF_6)_2$ and the corresponding electrochemical reactions (bottom). (A) Reduction of $[Pt(ppy)_2(bpy)](PF_6)_2$ accompanied by loss of the N^N ligand, (B) $[Pt(ppy)_2]^0/[Pt(ppy)_2]^-$ redox couple.

similar complexes containing a heavy metal and organic ligands was previously explored and proven to be a suitable method of computation with regards to the inclusion of the metal center. Coughlin et al. compared time-dependent computations using the LANL2DZ and 6-31G(d) basis sets for a Zn hemicage complex and found that, contrary to initial supposition, the larger basis set did not yield better results.[60] Indeed, LANL2DZ modeled the $\pi-\pi^*$ transition energies more accurately and was thus utilized for this study. Harmonic frequency calculations of $[Pt(ppy)_2(bpy)]^{2+}$ confirmed that the optimized structure was a minimum (see Supporting Information).

Orbital population analysis utilizing the singlet and triplet geometries indicated that luminescence should arise from a Ligand to Ligand Charge Transfer (LLCT) state, in which the highest occupied molecular orbital (HOMO) resides primarily on the C^N ligand and the lowest unoccupied molecular orbital (LUMO) involves

(52) Costa, R. D.; Viruela, P. M.; Bolink, H. J.; Orti, E. *J. Mol. Struct. THEOCHEM*. **2009**, *912*, 21.
(53) Chassot, L.; Muller, E.; Von Zelewsky, A. *Inorg. Chem*. **1984**, *23*, 4249.
(54) Ghavale, N.; Wadawale, A.; Dey, S.; Jain, V. K. *J. Organomet. Chem*. **2010**, *695*, 1237.
(55) Yamaguchi, T.; Kubota, O.; Ito, T. *Chem. Lett*. **2004**, *33*(2), 190.
(56) Choi, S.; Filotto, C.; Bisanzo, M.; Delaney, S.; Lagasee, D.; Whitworth, J. L.; Jusko, A.; Li, C.; Wood, N. A.; Willingham, J.; Schwenker, A.; Spaulding, K. *Inorg. Chem*. **1998**, *37*, 2500.
(57) Choi, H.-K.; Terzis, A.; Stevens, R. C.; Bau, R.; Haugwitz, R.; Narayanan, V. L.; Wolpert-DeFilippes, M. *Biochem. Biophys. Res. Commun*. **1988**, *156*(3), 1120.
(58) Choi, S.; Mahalingaiah, S.; Delaney, S.; Neale, N. R.; Masood, S. *Inorg. Chem*. **1999**, *38*, 1800.
(59) Brown, K. N.; Hockless, D. C. R.; Sargeson, A. M. *J. Chem. Soc., Dalton Trans*. **1999**, 2171.
(60) Coughlin, F. J.; Oyler, K. D.; Pascal, R. A., Jr.; Bernhard, S. *Inorg. Chem*. **2008**, *47*, 974.

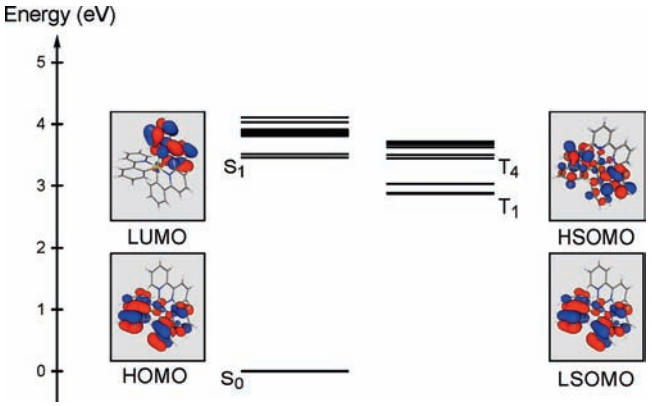

Figure 5. Energy level diagram showing the first 10 excited states in both the singlet and the triplet manifolds for $[Pt(ppy)_2(bpy)]^{2+}$. The lowest singly occupied molecular orbital (LSOMO) and highest singly occupied molecular orbital (HSOMO) differ from the highest occupied molecular orbital (HOMO) and lowest unoccupied molecular orbital (LUMO), respectively, because of intersystem crossing to the ^{3}LC state in lieu of the ^{3}LLCT.

almost exclusively the N^N ligand, both having slight metal character (Figure 5).

Clearly, since the experimental data revealed that the N^N ligand does not affect the emission energy of the complexes, its frontier orbitals do not strongly contribute to the emissive state. Therefore TD-DFT calculations were undertaken to model UV−vis absorption and investigate the discrepancy between the experimentally observed photophysical properties and the initial computations.

The absorption spectrum obtained from time-dependent computations in the singlet state carried out on $[Pt(ppy)_2(bpy)]^{2+}$ closely resembled the experimental trace (Figure 6). A ^{1}LLCT state, involving the HOMO and LUMO, was found again to be the lowest energy excited state (S_1) as shown by static calculations. However, the oscillator strength for this transition was low ($f = 0.0014$). The first transition with appreciably high oscillator strength involved S_3 ($f = 0.1091$) which was predominately a ^{1}LC $\pi \rightarrow \pi^*$ transition on the C^N ligand, and corresponded to the lower energy shoulder of the primary absorption band. The main transition of this band corresponding to S_{15} ($f = 0.3574$) was predicted to be a charge transfer mainly from the C^N ligand to the N^N ligand with a slight degree of metal character.

In contrast, time-dependent triplet calculations showed the lowest triplet state (T_1) to be ^{3}LC in character involving the C^N ligand and having a large singlet−triplet stabilization energy of 0.58 eV. The triplet state associated with S_1 was the fourth lowest in energy (T_4) and was 0.57 eV higher in energy than T_1. Thus, the computational data corroborate the experimental results. So in describing the excited state dynamics of this family of complexes it can be concluded that after absorption takes place into a mixed ^{1}LC-^{1}LLCT state, intersystem crossing occurs into the ^{3}LC state from which phosphorescence is observed.

Expansion of the Library. Additional synthetic work was undertaken to further examine the excited-state characteristics and extent of possible influence upon quantum yield in this new family of Pt^{IV} complexes. The library was expanded to include complexes of the

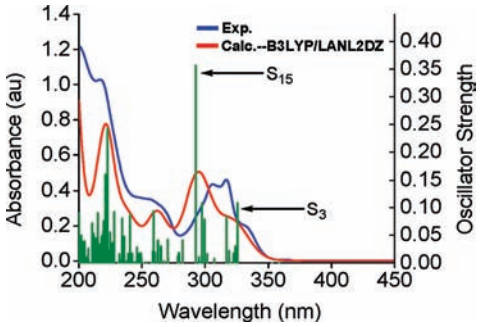

Figure 6. Experimental and calculated absorption spectra of $[Pt(ppy)_2(bpy)]^{2+}$. Calculated oscillator strengths are shown as green vertical lines; the transition to the excited states S_1 (the HOMO−LUMO transition) and S_2 cannot be seen because of low oscillator strength. The notable excited states S_3 and S_{15}, described in the text, are labeled above.

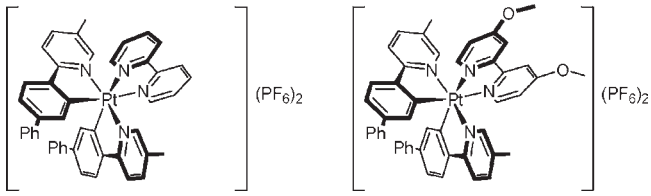

Figure 7. (**3j**) $[Pt(Ph\text{-}mppy)_2(bpy)](PF_6)_2$ and (**3k**) $[Pt(Ph\text{-}mppy)_2(dMeObpy)](PF_6)_2$.

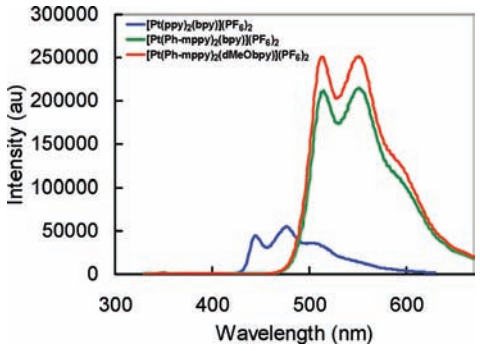

Figure 8. Relative intensities of emission of $[Pt(ppy)_2(bpy)](PF_6)_2$, $[Pt(Ph\text{-}mppy)_2(bpy)](PF_6)_2$, and $[Pt(Ph\text{-}mppy)_2(dMeObpy)](PF_6)_2$.

C^N ligand 5-methyl-2-(biphen-4-yl)pyridine (Ph-mppyH) for its extended π-system in hopes of increasing quantum yield and influencing the emission color . Derivatives incorporating bpy and dMeObpy were synthesized as before (Figure 7) and photophysical characterization yielded results that highlight the complexity of the interaction between excited states in these luminophores.

Luminescence profiles of the Ph-mppy derivatives were similar to the six previously described emissive Pt^{IV} complexes exhibiting a structured emission arising from a $\pi \rightarrow \pi^*$ transition on the C^N ligand. Quantum yields, 1.7% and 3.5% for the bpy and dMeObpy complexes respectively, out-shone the luminophores of the initial library (~1%) and are comparable to $[Ru(bpy)_3]^{2+}$ derivatives and $[Ir(ppy)_2(bpy)]^+$. The emission maxima were strongly red-shifted to 551 nm (Figure 8), while lifetimes increased more than 11-fold to 163 and 260 μs for the bpy and dMeObpy complexes, respectively (Table 4), which is in stark contrast to the Energy Gap Law. A plot of the natural log of the non-radiative rate constant (k_{nr}) versus

Table 4. Photophysical Data for the Expanded Library

complex	absorption[a] λ_{max}(nm)	emission[b] λ_{max}(nm)	$k_{nr}(10^3 s^{-1})$	$T^b(\mu s)$	Φ^c (%)	$K_{SV}[O_2]^b(mbar^{-1})$
(3j) $[Pt(Ph\text{-}mppy)_2(bpy)](PF_6)_2$	316 (2.85), 348 (2.66)	515, 551, 593 (sh)	0.603	163.10 ± 0.03	1.84 ± 0.09	1.84 ± 0.09
(3k) $[Pt(Ph\text{-}mppy)_2(dMeObpy)](PF_6)_2$	290 (3.29), 348 (2.73)	513, 551, 593 (sh)	0.371	259.65 ± 0.02	3.50 ± 0.18	2.12 ± 0.13

[a] Absorption data were measured in acetonitrile solution at room temperature. Molar extinction coefficients (ε) in 10^4 M^{-1} cm^{-1} are listed in parentheses. [b] Emission spectra and excited-state lifetimes were measured in acetonitrile solution at room temperature after bubbling with argon for 10 min; lifetimes were measured with a N_2 laser (3.5 ns pulse). [c] Quantum yields were calculated using $[Ru(bpy)_3](PF_6)_2$ as the reference standard.[49]

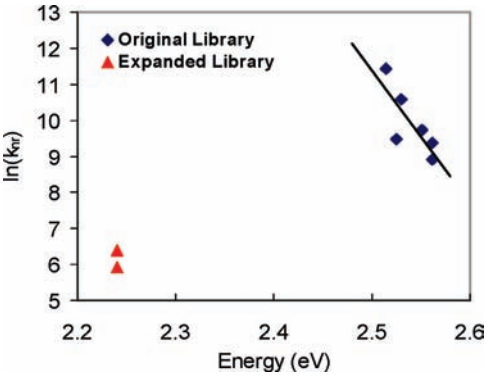

Figure 9. Energy-gap plot of the eight emissive Pt^{IV} complexes. The blue diamonds represent the complexes from the original library. The red triangles represent the Ph-mppy complexes, the change in the nature of the excited state of which is evident from their non-adherence to the Energy-Gap Law.

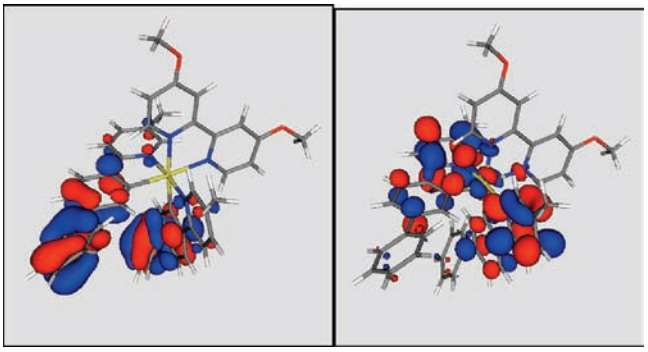

Figure 10. Orbitals depicting the predicted emissive ^{3}ILCT state of $[Pt(Ph\text{-}mppy)_2(dMeObpy)]^{2+}$. Left: lowest singly occupied molecular orbital (LSOMO); Right: highest singly occupied molecular orbital (HSOMO).

emission energy for all eight emissive Pt^{IV} complexes documenting this change is shown in Figure 9. The six original luminophores adhere to the expected trend of the Energy Gap Law, while the two Ph-mppy complexes do not.

Initial DFT calculations performed on $[Pt(Ph\text{-}mppy)_2(dMeObpy)](PF_6)_2$ also predict a different emissive state than that of $[Pt(ppy)_2(bpy)](PF_6)_2$. Static and time-dependent results of the singlet state showed similar frontier orbitals to those of the latter. However, time-dependent calculations of the triplet state show the lowest energy excited state not to be a simple ^{3}LC state, but an intraligand charge transfer state (^{3}ILCT) where the LSOMO resides on the two phenyl rings and the HSOMO resides on the pyridine and cyclometalated phenyl rings (Figure 10). This change in the nature of the excited state is a possible and likely explanation for why the Ph-mppy complexes exhibit such different luminescent properties and do not adhere to the Energy Gap Law as do the other complexes.

Table 5. Electrochemical Data for the Heteroleptic Pt^{IV} Bis-Cyclometalated Ph-mppy complexes[a]

complex	$E_{pc}Pt^{IV}/Pt^{II}$ (V vs SCE)	$E_{1/2}Pt^{II}(ppy)_2$ (V vs SCE)	ΔE_p (mV)
(3j) $[Pt(phmppy)_2(bpy)](PF_6)_2$	−1.027	−1.921	67
(3k) $[Pt(phmppy)_2(dmeobpy)](PF_6)_2$	−1.050	−1.918	83

[a] Measurements were taken of 400 μM solutions of the complex in acetonitrile after bubbling with N_2 for 5 min. Tetrabutylammonium Hexafluorophosphate (TBAH) was used as the supporting electrolyte at a concentration of 0.1 M. The experimental apparatus included a 1 mm^2 platinum working electrode, a platinum coil counter electrode, and a silver wire pseudo-reference electrode; ferrocene was used as an internal standard referenced against SCE at 0.371 V.

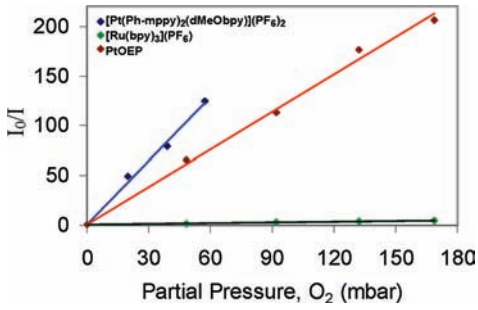

Figure 11. Stern−Volmer plot of $[Pt(Ph\text{-}mppy)_2(dMeObpy)](PF_6)_2$, PtOEP, and $[Ru(bpy)_3](PF_6)_2$. $[Pt(Ph\text{-}mppy)_2(dMeObpy)](PF_6)_2$ is shown to demonstrate superior quenching. Measurements were taken in a 1 cm quartz cuvette using 15 μM solutions of the complex in acetonitrile, bubbling with Argon/Oxygen mixtures for 10 min prior to the measurement with an excitation wavelength of 317 nm.

Further elucidation by the study of structure/property relationships and additional computations is ongoing.

Electrochemical characterization provided more confirmation to the trends observed previously (Table 5), while solvatochromic studies of $[Pt(Ph\text{-}mppy)_2(dMeObpy)](PF_6)_2$ once again showed no shift of emission maxima in the same range of solvents that were used for earlier studies.

It was discovered that $[Pt(Ph\text{-}mppy)_2(bpy)](PF_6)_2$ **(3j)** and $[Pt(Ph\text{-}mppy)_2(dMeObpy)](PF_6)_2$ **(3k)** were highly sensitive to oxygen quenching; at oxygen concentrations of 5% only minimal luminescence can be observed for either complex. Therefore, their rates of quenching were compared to that of $[Ru(bpy)_3](PF_6)_2$ and platinum^{II} 2,3,7,8,12,13,17,18-octaethyl-21*H*,23*H*-porphyrin (PtOEP), two standards in the field of luminescent sensors[18,51] (Figure 11). $[Ru(bpy)_3](PF_6)_2$ and PtOEP demonstrate long phosphorescence lifetimes (0.938 and 50 μs respectively) and sensitivity to oxygen quenching (K_{SV} = 0.024 $mbar^{-1}$ and 1.254 $mbar^{-1}$, respectively). It was found that **(3j)** and **(3k)** demonstrate superior quenching to that of either $[Ru(bpy)_3](PF_6)_2$ or PtOEP with K_{SV} values of 1.796 $mbar^{-1}$ and 2.126 $mbar^{-1}$ respectively. This is due primarily to the longer lifetimes and favorable energy-transfer energetics of these complexes,

both of which are essential for application in sensor technology.

Conclusions

Presented is a library of the first heteroleptic bis-cyclometalated Pt^{IV} complexes of the architecture $[Pt(C^N)_2(N^N)](PF_6)_2$ which have been fully characterized with photophysical, electrochemical, and spectroscopic methods. Because of the large ligand field splitting of the Pt^{IV} ion, the photoluminescence of the complexes is highly blue-shifted exhibiting emission maxima as low as 482 nm. The most prominent feature in the cyclic voltammogram is an irreversible reduction from Pt^{IV} to Pt^{II}, leading to ligand dissociation, followed by a one-electron reduction of the resulting bis-cyclometalated Pt^{II} species. The ^{3}LC character of the excited state, observed in photophysical measurements, was elucidated by static and time-dependent density-functional theory calculations which showed that the singlet−triplet stabilization energy for the ^{3}LC state was significantly greater than that of the ^{3}LLCT state, the lowest-lying excited state initially expected to be the source of phosphorescence.

The initial library of complexes showed a long-lived excited state, upward of 15 μs and quantum yields reaching 1%. The elucidated structure−property relationships were used to synthetically change the emission properties of two additional complexes. A shift of emission energies of 70 nm and an 11-fold increase in quantum yield compared to $[Pt(ppy)_2(bpy)](PF_6)_2$ was attained in the Ph-mppy derivatives. Moreover, the long-lived triplet states (lifetimes as high as 260 μs) of these complexes demonstrate a high sensitivity to oxygen quenching with K_{SV} values up to 2.12 $mbar^{-1}$. The discovered structure−property relationship is now being judiciously explored to tailor materials for optical oxygen sensors, LECs, and other luminescence-based applications.

Supporting Information Available: Further details about the synthetic procedures and characterizations, ^{1}H NMR spectra for complexes (**3a**)−(**3k**), information about the DFT calculations, and complete citation of reference 50. This material is available free of charge via the Internet at http://pubs.acs.org.